Title: Black carbon concentrations and modeled smoke deposition fluxes to the bare ice dark zone of the Greenland Ice Sheet

Authors: Alia L. Khan[1], Peng Xian[2], Joshua Schwarz[3]

[1]Department of Environmental Sciences, Western Washington University

[2]Aerosol and Radiation Section of the Marine Meteorology Division, Naval Research Laboratory, Monterey, California, USA

[3]Chemical Sciences Division, NOAA Earth System Research Laboratory (ESRL), Boulder, CO, United States

***Correspondence to*:** Alia L. Khan (alia.khan@wwu.edu)

Abstract:

Ice-albedo feedbacks in the ablation region of the Greenland Ice Sheet (GrIS) are difficult to constrain and model due in part to our limited understanding of the seasonal evolution of the bare-ice region. To help fill observational gaps, 13 surface samples were collected on the GrIS across the 2014 summer melt season from patches of snow that were visibly light, medium, and dark colored. These samples were analyzed for their refractory black carbon (rBC) concentrations and size distributions with a Single Particle Soot Photometer coupled to a characterized nebulizer. We present a size distribution of rBC in fresh snow on the GrIS, as well as from surface hoar in the bare ice dark zone of the GrIS. The size distributions from the surface hoar samples appear unimodal, and were overall smaller than the fresh snow sample, with a peak around 0.3 μm. The fresh snow sample contained very large rBC particles that had a pronounced bimodality in peak size distributions, with peaks around 0.2 μm and 2 μm. rBC concentrations ranged from a minimum of 3 μg-rBC/L-H_2O in light-colored patches at the beginning and end of the melt season, to a maximum of 32 μg-rBC/L-H_2O in a dark patch in early August. On average, rBC concentrations were higher (20 μg-rBC/L-H_2O ± 10 μg-rBC/L-

H_2O) in patches that were visibly dark compared to medium patches (7 µg-rBC/L-H_2O ± 2 µg-rBC/L-H_2O) and light patches (4 µg-rBC/L-H_2O ± 1 µg-rBC/L-H_2O), suggesting BC aggregation contributed to snow aging on the GrIS, and vice versa. Additionally, concentrations peaked in light and dark patches in early August, which is likely due to smoke transport from wildfires in Northern Canada and Alaska as supported by the Navy Aerosol Analysis and Prediction System (NAAPS) reanalysis model. According to model output, 26 mg/m^3 of biomass burning derived smoke was deposited between April 1st and August 30th, of which 85% came from wet deposition and 67% was deposited during our sample collection timeframe. The increase in rBC concentration and size distributions immediately after modelled smoke deposition fluxes suggest biomass burning smoke is a source of BC to the dark zone of the GRIS. Thus, the role of BC in the seasonal evolution of the ice-albedo feedback should continue to be investigated in the bare-ice zone of the GrIS.

1. Introduction

The bare ice dark zone of the southwest Greenland Ice Sheet (GrIS) is characterized by low albedo due in part to the presence of light absorbing impurities (LAIs), that create a positive ice-albedo feedback through increased surface melting, ice grain growth, and darkening (Tedesco et al., 2016). LAIs in this region are a mixture of cryoconite, ice algae (Stibal et al., 2017; Ryan et al., 2018), dust (Wientjes et al., 2011), and black carbon (BC) such as from Northern Hemisphere fires (Khan et al., 2017a), yet the relative contribution of each light absorbing particle is still uncertain. The radiative forcing of these LAIs, along with warming summer surface temperatures (Hanna et al., 2008), leads to large volumes of supra-glacial melt (Greuell, 2000). Furthermore, retreat of the snowline is amplifying surface melt of the GrIS due to

increased bare ice exposure (Ryan et al., 2019) and the LAI-ice albedo feedbacks described above.

BC in and on snow and ice is known to warm the Arctic and contribute to snow and ice melting, however the magnitude of its influence is still highly uncertain e.g., (Flanner et al., 2007; Bond et al., 2013). BC concentration in air is typically operationally defined depending on the analytical technique used (Petzold et al., 2013). Many in-situ measurements of BC concentration in snow in the Arctic have been reported by the Integrating Plate and Integrating Sandwich (IS) technique, which provides analysis of light absorption of particulate impurities through spectrophotometric analysis of filter loaded with particulates collected from melted samples (e.g., Clarke and Noone, 1985; Doherty et al., 2010; Doherty et al., 2013). Doherty et al. (2010) reported a median concentration of 3 ng/g in surface snow, with higher concentration layers up to ~20ng/g in snow profiles at Dye 2. Snow samples from snowpits in the northwest sector of the GrIS were also collected in 2013 and 2014 from two traverses and analyzed for elemental/organic carbon (EC/OC). The mean concentration of the samples collected was 2.6 ng/g and the mean peak was 15 ng/g. Based on these results, it was determined that EC/OC do not influence the snow albedo in the NW sector of the GrIS dry zone (Polashenski et al., 2015a). Observations of refractory black carbon (rBC) analyzed by the Single Particle Soot Photometer (SP2) have been published from snow profiles and ice cores in the accumulation region closer to the Summit research station (McConnell et al., 2007a; Keegan et al., 2014b; Lim et al., 2014). McConnell et al. (2007) presented BC concentrations from a 215-year ice-core record collected at D4 in West Central Greenland with average concentrations of 1.7ng/g in pre-industrial times, 2.3ng/g over the period 1950-2002, and around 5 ng/g in the peak period of the early 1900s. The maximum monthly concentration observed was 58.8 ng/g in 1854, however, monthly

74 concentrations only exceeded 5 ng/g ~2-3 times each decade after 1950. Polashenski et al.,
75 (2015) provides a comprehensive review of previous BC concentrations in their supplemental
76 info, showing that the BC average ranges between 1.5 and 3 ng/g over an annual cycle, with peak
77 deposition occurring during summer episodic events, with concentrations of 5 - 10+ ng/g only
78 occurring a few times at a given site per decade. Similarly, rBC concentrations from the
79 percolation zone of the GrIS have been shown to be relatively low, less than 1.5 ng/g (Lewis et
80 al., 2021).
81 rBC measured by SP2 has been shown to provide more reliable measurements of
82 concentration than the IS or EC/OC (from liquid and air samples, respectively) techniques
83 because it is largely free from the interference of materials other than rBC (Kondo et al., 2011;
84 Schwarz et al., 2012) such as pyrolyzed organic carbon artifacts (Lim et al., 2014). It also
85 provides a lower detection limit and increased sensitivity at low concentrations (Lim et al. 2014).
86 The SP2 coupled with a nebulizer also provides a measurement of rBC particle size distribution
87 from liquid samples.
88 rBC particle size has been observed in some snow samples to be larger than expected
89 from atmospheric measurements, reflecting to some degree size-dependent removal processes
90 from the atmosphere (Schwarz et al., 2013). The rBC size distribution in snow, which at this
91 point is constrained by direct observations not supported by detailed modeling, is a significant
92 source of uncertainty for calculating the overall radiative forcing of BC-in-snow on the Arctic
93 climate, as well as the global climate (e.g., Bond et al., 2013). Very few rBC size distributions in
94 snow have been reported globally, with most measurements coming from the Arctic (Lim et al.,
95 2014; Khan et al., 2017b; Mori et al., 2019).

Although, observations of BC in snow have been previously observed in the percolation zone (Dye 2) and accumulation zone (Summit Station) by the IS technique (Doherty et al., 2010, 2013) and rBC-SP2 at Summit Station (McConnell et al., 2007b; Keegan et al., 2014a; Lim et al., 2014), to the authors' knowledge, no reports of rBC concentrations with size distributions in snow and surface hoar have been reported from the GrIS, providing new insight, particularly into the dynamic bare-ice region.

Here we present rBC concentrations with size distributions from the bare ice region of the GrIS before and after influence by a major wildfire event, along with NAAPS modelled wet and dry deposition. Our findings suggests that rBC surface hoar concentrations in the bare ice zone reflect atmospheric conditions momentarily, before being reset, possibly by supra-glacial melt. Additionally, NAAPS model output suggest most of the biomass burning derived smoke deposition comes in the form of wet removal (i.e., removal by precipitation). These rBC concentrations and size distributions provide insight into the seasonal evolution of impurities, which are needed to constrain ice-albedo feedbacks in the bare-ice zone of the GrIS.

2. Methods

2.1 Site Description and Snow Sampling

The field site was in the southwestern region of the GrIS near the S6 automated weather station at 67 04.779'N, 49 24.077'W, and 1011 m above sea level. More information on the study site can be found in Stibal et al. (2017). A fresh snow surface sample (2 – 3 cm), was collected just after a snow event on 2014-06-27. Three surface hoar samples (2 – 3 cm), were collected in 150 mL pre-cleaned and combusted amber glass bottles four times between 2014-06-28 and 2014-08-11 across the 2014 summer melt season from visually identified light, medium, and dark patches

of surface hoar, for a total of 13 samples, including the fresh snow. While all sample sites could include a mixture of ice algae, dust, black carbon (i.e, cryoconite), the dark patches especially could represent refrozen melt that is enhanced in LAIs, including rBC. A mixture of light, medium and dark 1 – 3 m^2 patches were sampled within the ~.5 km^2 study area to characterize the breadth of surface types and heterogenous distribution of impurities. Samples were stored frozen in a 'field cooler' dug into the ice and then transported frozen on ice to Kangerlussuaq, and shipped on dry ice to the Denver Airport, and then transported immediately to a freezer at the Institute of Arctic and Alpine Research (INSTAAR) at the University of Colorado – Boulder.

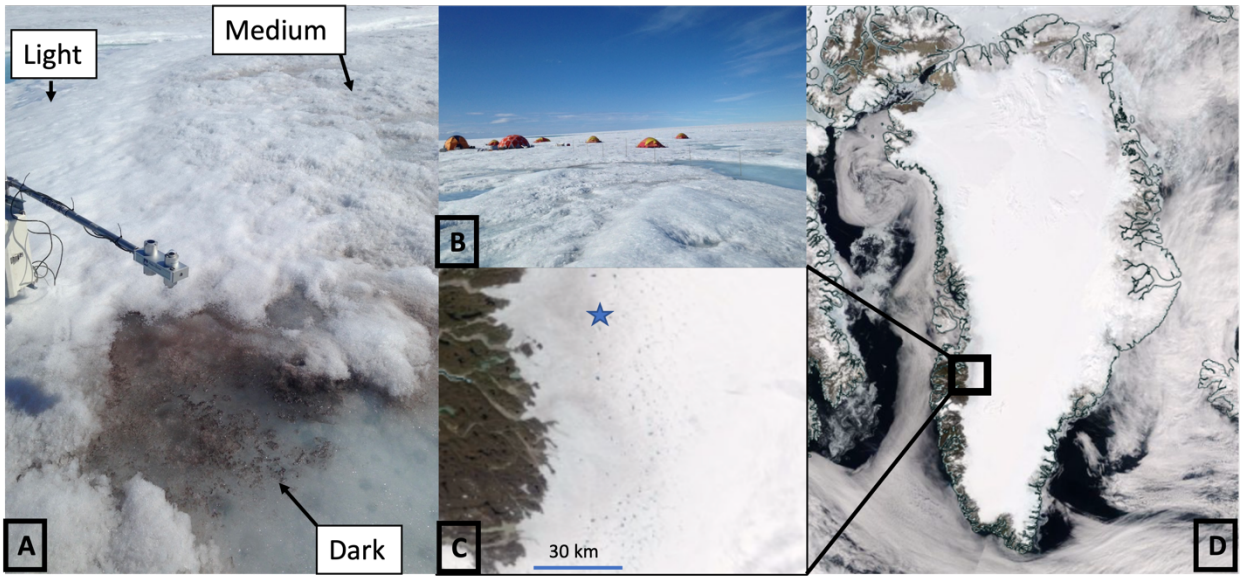

A and B are images collected by Dr. Alia Khan. C and D are MODIS satellite images acquired from the NASA Worldview application.

Figure 1: A) Example light, medium and dark patches of ice. B) The Dark Snow Field Camp. C) The southwest GrIS dark zone with the field sampling location indicated by a blue star and D) the GrIS from MODIS on July 2nd, 2014.

2.2 Processing for Refractory Black Carbon

The samples were transported frozen from INSTAAR to the Earth System Research Laboratory at the National Oceanic and Atmospheric Administration where they were analyzed for rBC

mass mixing ratios (MMRs) by SP2 coupled to a nebulizer per the methods described in Katich et al. (2017) and Khan et al. (2018). Briefly, the samples were melted for the first time just prior to analysis with the SP2 and aerosolized with a carefully calibrated concentric pneumatic nebulizer based on a customized U5000 AT+ nebulizer (Teledyne Cetac, Inc.) which the ultrasonic piezo was replaced with a concentric pneumatic nebulizer. The SP2 was calibrated with fullerene soot (Lot# F12S011, Alfa Aesar Inc., Wood Hill, MA) with the community calibration approach (Baumgardner et al., 2012) over masses of 1 – 20 fg. Using a power law calibration dependence following Schwarz et al., [2012], the resulting linear calibration of SP2 signal to rBC mass applied to mass of 80 fg was extended further to 4000 fg. The SP2 was operated with a widely staggered gain for two incandescent channels, allowing sizing of rBC mass in the range ~1 – 4000 fg.

Melted snow samples were interspersed with deionized water blanks to confirm a low background, especially relative to the MMRs, indicating no appreciable contamination to concentrations and size distributions. Little size-dependence in nebulization efficiency was confirmed with concentration standards of polystyrene latex spheres (PSLs) over 220 – 1500 nm diameter, which is consistent with recent results from concentric pneumatic nebulizers (Wendl et al., 2014, Katich et al., 2017). Therefore, size dependent corrections were not necessary. During data acquisition with the SP2, its lower mass-detection limit was 1.2 fg, which corresponds to about a 110 nm volume equivalent diameter (VED) size detection limit, assuming 1.8g/cc void free density. A 510 nm diameter PSL concentration standard was sampled between melted snow analyses to track possible changes in nebulization efficiency during each day of sampling. This revealed effectively constant efficiency varying with a standard deviation less than 5%. A gravimetric mass concentration standard (Schwarz et al., 2012) was also used to evaluate

158 nebulization efficiency. The results of the PSL and gravimetric calibrations of nebulizer
159 efficiency were consistent within uncertainties of 20% and were averaged to provide a best-
160 estimate nebulization efficiency that was then used to produce the BC MMR values as in
161 Schwarz et al. (2012).
162
163 2.3 *Global Aerosol Modeling*
164 The Navy Aerosol Analysis Prediction System (NAAPS) model is a global aerosol transport
165 model which provides 6-hrly biomass burning smoke, anthropogenic and biogenic fine aerosols,
166 dust, and sea salt aerosol forecasts and analyses below 100 hPa at 1/3^{o} latitude/longitude spatial
167 resolution and contains 42 vertical atmospheric levels. The NAAPS reanalysis (NAAPS-RA) is
168 available 2003-current with a coarser spatial resolution (1^{o} latitude/longitude horizontal and 25
169 vertical levels) (Lynch et al., 2016). Total column aerosol optical thickness (AOT) is constrained
170 through assimilation of quality-controlled satellite AOT retrievals from the Moderate Resolution
171 Imaging Spectroradiometer (MODIS) and Multi-angle Imaging SpectroRadiometer (MISR).
172 Near-real time satellite based thermal anomaly data enables detection of wildfires and
173 construction of biomass burning smoke emissions (Reid et. al., 2009). Orbital corrections for
174 MODIS-based fire detections and regional factors were applied on emissions so that the
175 reanalysis AOT verifies well with ground-based measurements (Lynch et al., 2016). The
176 NAAPS-RA has been applied to a broad range of science applications, and specifically the life
177 cycle, climatology, radiative forcing, aerosol-atmosphere-ice-ocean interactions of biomass
178 burning smoke aerosols (e.g., Reid et al., 2012; Xian et al., 2013; Markowicz et al., 2021; Ross et
179 al., 2018; Khan et al., 2019; Carson-Marquis et al., 2021), as well as previously to corroborate
180 wildfire smoke transport to the GrIS (Khan et al., 2017a), Arctic Canada (Ranjbar et al., 2019),

Svalbard (Markowicz et al., 2016; 2017), the pan-Arctic region (Xian et al., 2022a, b), the Nepalese Himalayas (Khan et al., 2020), and the Antarctic (Khan et al., 2018; Khan et al., 2019). Speciated AOT, surface aerosol concentration and deposition flux are used in this study. Here the deposition is calculated as 24-hour flux to the surface of the ice sheet in mg/m^2/day. Estimating atmospheric properties related to biomass burning is highly complex and is influenced by wide variety of factors such as the type of fuel, combustion temperature, and atmospheric conditions. Also, the chemical, optical and physical properties of biomass burning aerosols can change during atmospheric transport and dispersion. The mass ratio of rBC to total mass in biomass burning smoke particles is estimated to be 5–10% black carbon in the NAAPS-RA model based on field studies (see a summary in Reid et al., 2005) and here we chose 7% as a median value.

3. Results and Discussion

3.1 rBC Concentrations

rBC concentrations in the surface hoar ranged from a minimum of 3 μg-rBC/L-H_2O in light patches at the beginning and end of the melt season, to a peak of 32 μg-rBC/L-H_2O in a dark patch in early August (Table 1). rBC concentrations were higher in patches that were visibly darker (20 μg-rBC/L-H_2O) compared to medium patches (7 μg-rBC/L-H_2O) and light patches (4 μg-rBC/L-H_2O), suggesting BC aggregates with dust and biological material on the GrIS. Light and dark patch concentrations peaked in early August. Our minimum concentrations are in the range of rBC concentrations found elsewhere on the GrIS, but our peaks are higher than previously reported concentrations from snow on the GrIS (Doherty et al., 2010; Polashenski et al., 2015; Lewis et al., 2021). Our maximum concentrations are higher than the highest concentrations observed in vertical snow with the IS (Doherty et al., 2010) and EC/OC technique

(Polashenski et al., 2015), but less than the highest monthly average concentration of year of 1854 reported in an ice core by McConnell et al. (2007). The concentration of rBC in the fresh snow (3 µg-rBC/L-H_2O) sample was roughly the same as the light surface hoar patches on 2014-06-28 and 2014-08-11.

Table 1: NAAPs Smoke Dry, Wet, and Total Deposition (mg/m^2/day) from April 1st prior to sample collection. Average rBC concentrations from visually light, medium, and dark patches of surface hoar. All samples were collected at 67.07979701 degrees N and -49.40116603 degrees W at 1005 meters above sea level in the dark zone ablation region of the SW Greenland Ice Sheet. ^The fresh snow sample is a single sample.

Date	**NAAPS Smoke Dry Deposition (mg/m^3/day)**	**NAAPS Smoke Wet Deposition (mg/m^3/day)**	**NAAPS Smoke Total Deposition (mg/m^2/day)**	**Average rBC** μg-rBC/L-H_2O	**Snow type (visual color)**	**rBC** μg-rBC/L-H_2O
6/27/14	0.58	1.98	2.56	3.05^	Fresh	3.05
6/28/14	0.60	6.92	7.51	8.37	Light	2.87
					Medium	9.61
					Dark	12.62
7/21/14	0.75	6.93	7.69	11.45	Light	4.21
					Medium	6.42
					Dark	23.71
8/2/14	1.51	9.44	10.95	14.15	Light	5.27
					Medium	4.71
					Dark	32.47
8/11/14	1.94	12.14	14.08	8.12	Light	2.96

	Medium	8.75
	Dark	12.64

214

215 *3.2 rBC Size Distributions*

216 We found very large rBC are present (Figure 2A, B and C), especially in the fresh snow sample.
217 The large size distribution in fresh snow follows previous findings in the rocky mountains that
218 rBC size distributions can be larger in surface snow than expected in aerosol in the atmosphere
219 (Schwarz et al., 2013). Furthermore, the fresh event is associated with a more pronounced
220 bimodality at ~ 0.2 μm and 2 μm (Figure 2A), whereas the rBC in surface hoar samples appears
221 more unimodal (Figure 2B and 2C). The average surface hoar rBC sizes, which have not been
222 previously reported in the literature, are smaller than the one fresh snow sample with a peak
223 around 0.3 μm. This is still larger than typical modal sizes for rBC observed in the atmosphere
224 (in the range ~0.11 – 0.2 μm typically). Furthermore, no apparent patterns emerge in the size
225 distributions across the light, medium and dark patches over the duration of the season.
226 However, the surface hoar rBC size distributions likely evolve, just as the seasonal snow cover
227 evolves into bare ice and surface hoar, but we are unable to assess from this relatively small data
228 set. This conjecture is supported by observations that repeated freeze/thaw cycles tend to cause
229 rBC coagulation in liquid (Schwarz et al., 2013). Regardless, these initial results of rBC size
230 distributions from fresh snow and surface hoar in the bare ice region of the GrIS are important
231 for informing ice-albedo models, which are still being developed and refined for bare ice regions
232 of the ice sheet (e.g. Flanner et al., 2007).

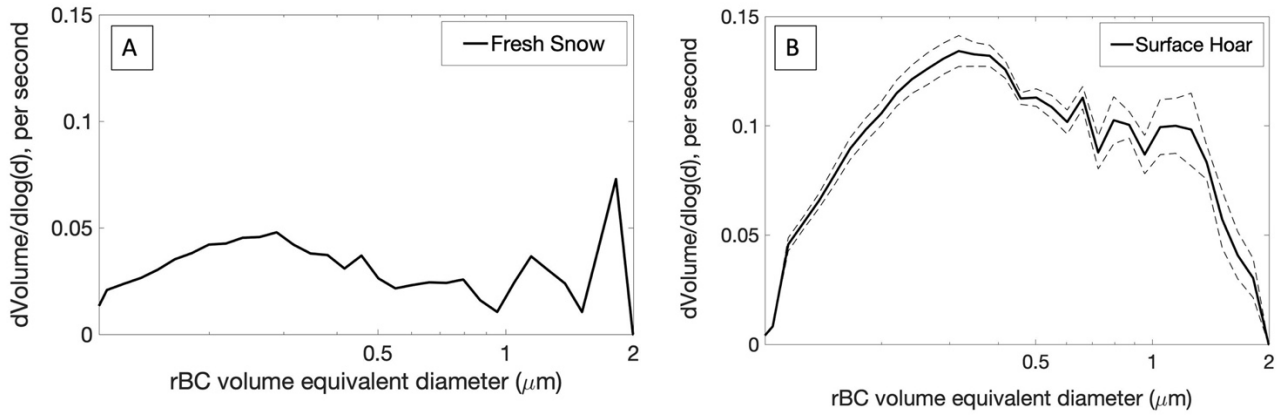

233

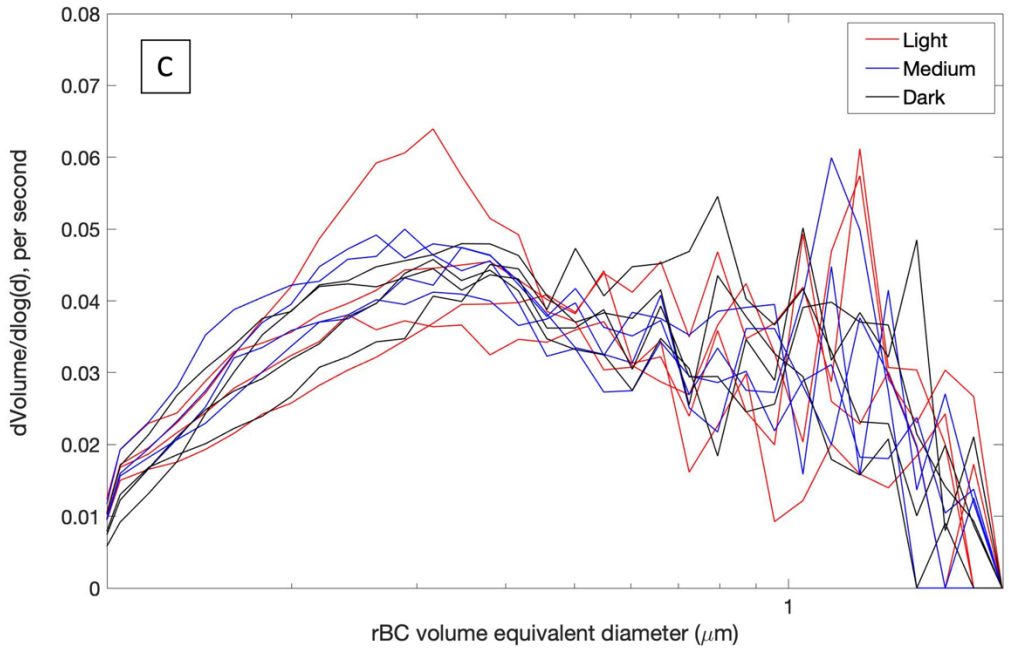

234

235 **Figure 2:** A) rBC size distribution of fresh snow (n=1), B) all surface hoar samples over the
236 duration of the season (n=12) and C) the size distribution of each surface hoar sample
237 categorized as light, medium and dark. The dashed lines in Figure 2B represent the max and min
238 size distributions and the solid black line is the average.

239

240 *3.3 NAAPS Aerosol Model Comparison and Evaluation*

The ground observations were then compared to cumulative aggregates of smoke deposition fluxes modelled with the Navy Aerosol Analysis Prediction System reanalysis model. AOT derived from MODIS and modeled by NAAPS demonstrates that a large wildfire smoke event was observed just before the third sample was collected and during the time the fourth sample was collected (Figure 3). Concomitant AOT and surface concentration predictions from the NAAPS model confirms our peak concentrations are likely due to Northern Hemisphere wildfire smoke (Figure 4 A- D).

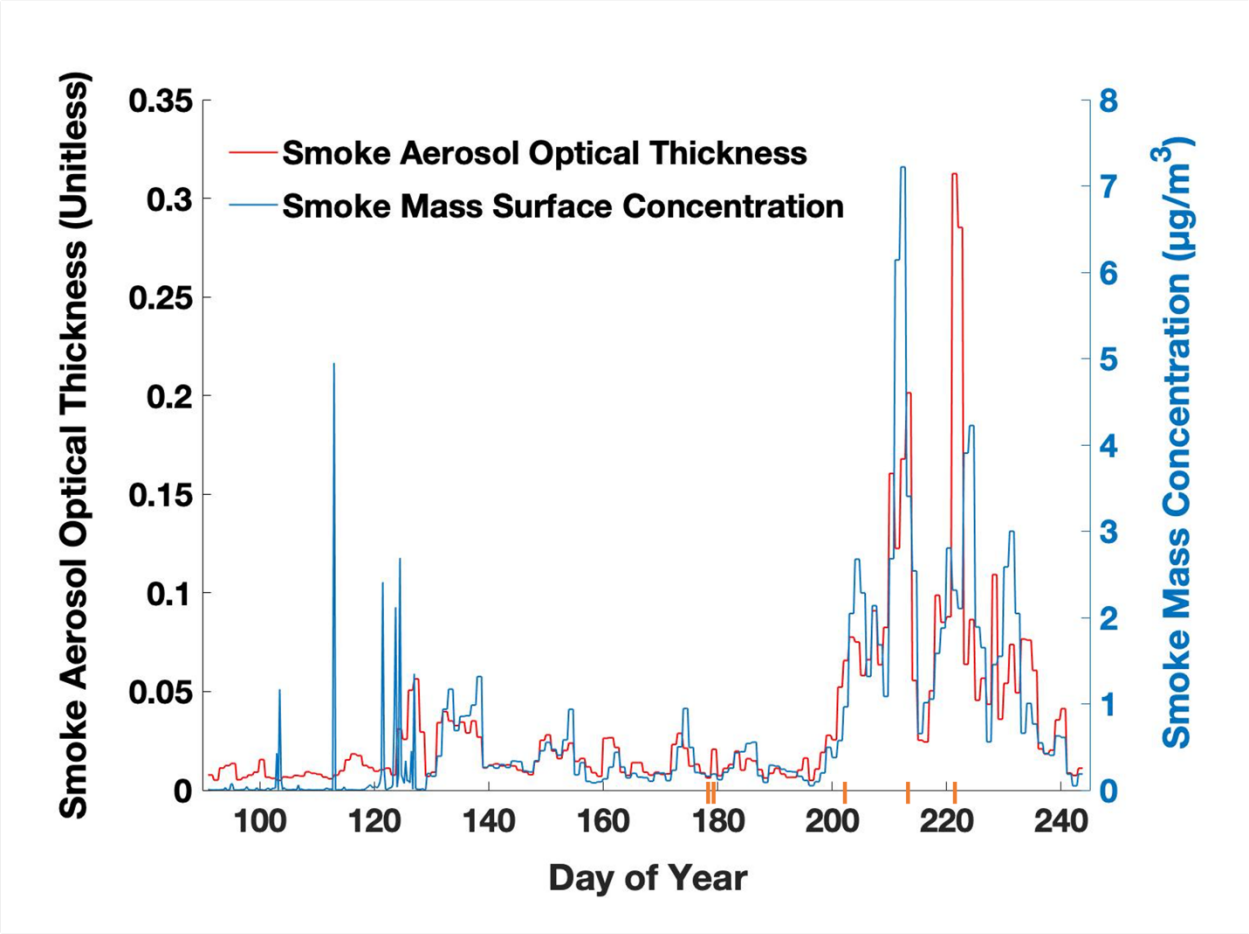

Figure 3: Aerosol optical thickness (AOT) derived from NAAPS reanalysis

over the sampling season from smoke and dust. B) Smoke mass concentration (μg/m^3) in the surface layer of the model (centered around 16m). The five sampling dates are marked in orange.

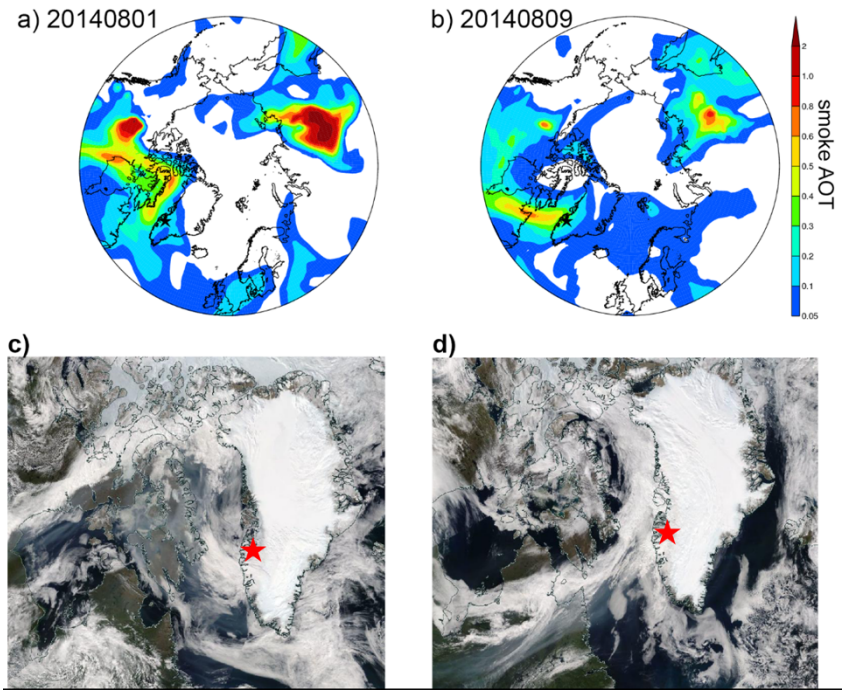

Figure 4: Biomass burning smoke transport reaching the GrIS from the west based on NAAPS-RA daily-mean smoke AOT and MODIS TERRA true color imageries for **A and C)** Aug. 1, 2014 and **B and D)** Aug. 9, 2014. The sampling location is marked with a black star in the NAAPS-RA plots (A and B), and red stars in the MODIS imageries (C and D).

According to NAAPS model output, the deposition flux of smoke (Table 1 and Fig. 5) onto the ice surface of the dark zone during our model study period, April 1st – August 30th, was 25.6 mg/m^2/day and 85% came from wet deposition. April 1st to August 30th was chosen based on the primary Northern Hemisphere wildfire season and smoke transport to the Arctic (Xian et al., 2022b). 68% of this smoke (17.3 mg/m^2/day) was deposited during our sample collection period from June 27th to August 11th. Prior to the first sample collected on June 27th, 10% of the total smoke flux (2.6 mg/m^2/day) was deposited from April 1st to June 26th. After the last sample was collected on August 11th, 5.8 mg/m^2/day of smoke was deposited between August 12th and 30th.

We evaluate the NAAPS-RA deposition flux based on the rBC concentration observed in fresh snow, which was 3 μg-rBC/L-H_2O. The NAAPS model assumes 7% of smoke is BC. The snow event that preceded the fresh snow sample collection, had a modeled precipitation rate of 10 mm/day or 10 L/m^2. The modeled smoke deposition flux is 3000 μg/m^2/day or 300 μg/L over 24 hours. At 7% BC of total smoke, that leaves us with 21 μg-BC/L-H_2O. Therefore, the model appears to be off by roughly a factor of 7 for this one snow sample. Continued work is in progress to evaluate the model across a larger sample size of rBC ground observations across the Arctic.

Two case studies of interest arise in the modelled total NAAPS smoke flux when comparing wet and dry deposition. The first one is a large wet deposition flux and the second is a considerable dry deposition flux. The first wet deposition flux occurred between June 27th and 28th (day of year 178 and 179), during a snow event (Fig. 5A and B). Here we see the largest increase in the total deposition flux of smoke over the study period at 5.0 mg/m^3/day in just over 24 hours. 99.8% of this comes from wet deposition. When we compare these model findings to the observational rBC data in the surface hoar and snow, we see the rBC concentration in fresh snow, 3 μg-rBC/L-H_2O, is high compared to pristine fresh snow previously found in Svalbard, 1 μg-rBC/L-H_2O (Khan et al., 2017b). The average rBC concentration across the light, medium and dark patches is also relatively high for a non-human impacted site in the polar regions (Cordero et al., 2022). A previous study of black carbon in supra-glacial melt from the same GRIS site previously confirmed the dissolved BC molecular signature was indicative of wildfire smoke that likely came from Northern Canada and Alaska (Khan et al., 2017a). Between July 22nd and August 2nd, the model again shows a large proportion of the total deposition flux coming from wet deposition, 77% of the 3.2 mg/m^2/day. Similarly, from August 3rd to 11th, 86%

290 of the 3.1 mg/m^3/day smoke deposition flux was from wet deposition (Fig. 5A). Again, this
291 follows an increase in the total precipitation (Fig. 5B).

292 However, a dry deposition case arises on July 21st, 2014 (DOY 172). Here the NAAPS
293 model does not produce a large total smoke deposition flux, but the rBC concentrations are still
294 relatively high. Since the previous sampling event on June 28th (DOY 179), the model produces
295 0.2 mg/m^3/day total deposition flux, where only 16% comes from wet deposition. The majority,
296 84%, is from dry smoke deposition. This finding is also supported by the fact that there was little
297 precipitation during this time based on the NAAPS modeled meteorology (Fig. 5B), but it is also
298 important to note that snow aging could also play a role in aggregation of BC particles. The
299 decrease observed in the surface hoar rBC concentrations in the August 11th samples may
300 suggest there was a process that removed the particles from the surface hoar, such as flushing or
301 redistribution by supra-glacial melt, or uncontaminated fresh snow deposition which could dilute
302 the concentrations. Further investigation into this process is warranted.

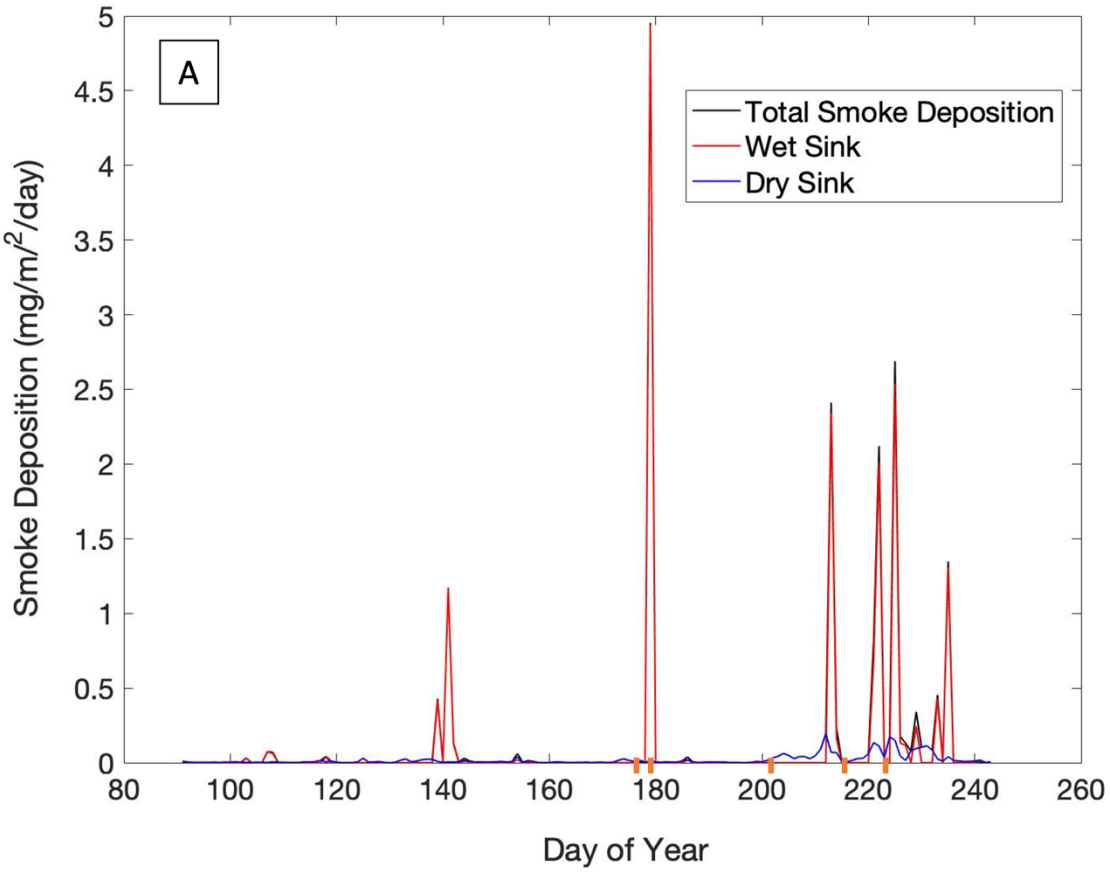
A
Total Smoke Deposition
Wet Sink
Dry Sink
Smoke Deposition (mg/m^2/day)
Day of Year
0
0.5
1
1.5
2
2.5
3
3.5
4
4.5
5
80
100
120
140
160
180
200
220
240
260

303

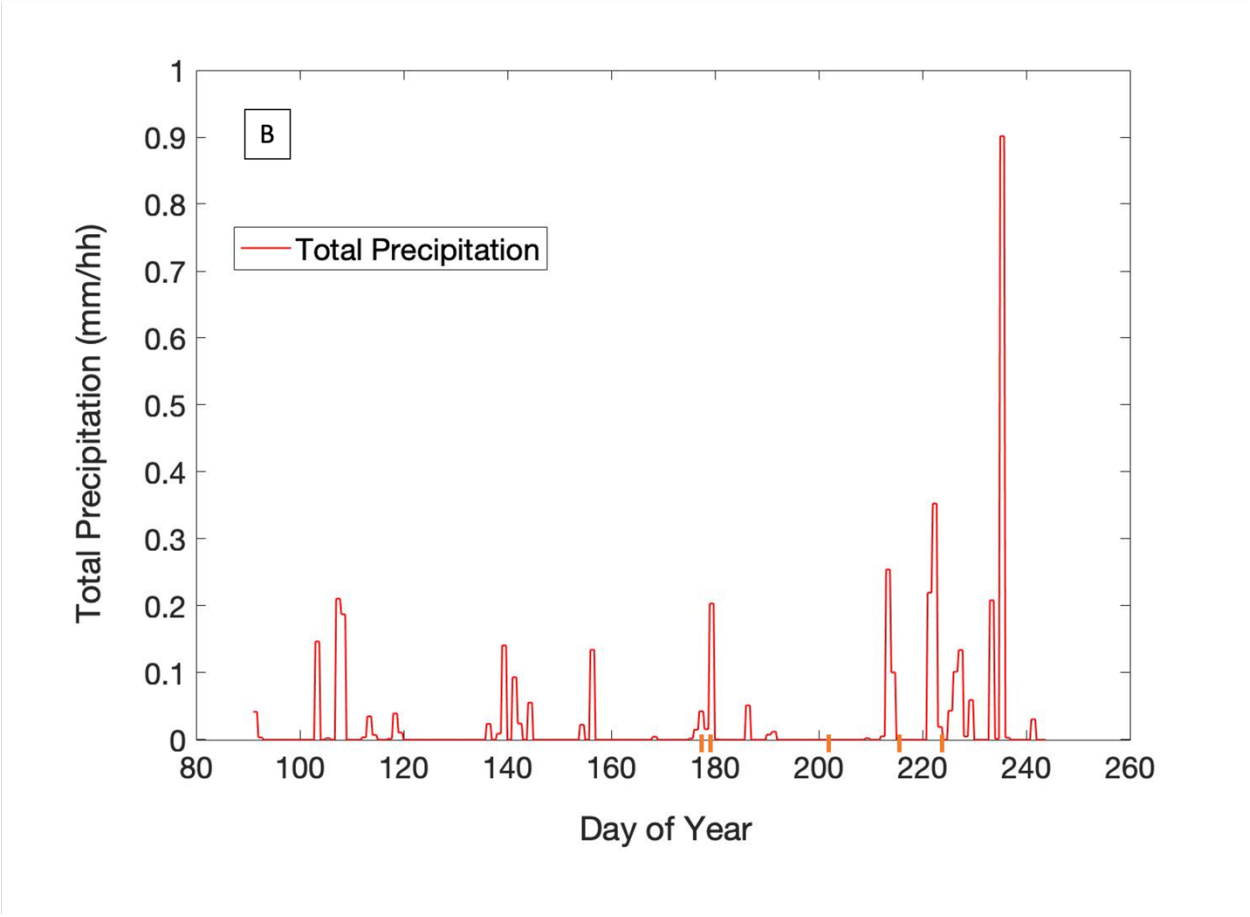

Figure 5: A) Biomass burning derived smoke deposition flux separated as wet and dry deposition and B) total precipitation produced by the NAAPS model. The total smoke deposition closely follows the wet deposition line. The five sampling dates are marked in orange.

4 Conclusion

Here we present (to the author's knowledge) the first rBC size distributions from fresh snow and surface hoar in the bare ice region of the GrIS, coupled with their concentrations. An initial rBC size distribution in a fresh snow sample from the GrIS shows pronounced bimodality and very large particles with the second peak almost 2 µm. These initial rBC size distributions from surface hoar in the bare ice dark zone of the Greenland Ice Sheet are smaller than the fresh snow, but still much larger than observations of atmospheric rBC. There appears to be a shift in the

316 modal peak of rBC particle size in light patches over the duration of the season from ~ 0.3 μm to
317 ~1.4 μm, further suggesting aggregation of particles in the bare-ice region. NAAPS-AOT and
318 surface concentration data suggest that rBC surface hoar concentrations in the bare ice zone
319 reflect atmospheric conditions momentarily, before possibly being reset by supra-glacial melt.
320 Additionally, we demonstrate preliminary verification of BC deposition from the NAAPS-
321 RA with *in-situ* observations. rBC measurements in dark patches from late June to early August
322 2014 reveal an increase just after the smoke event. These elevated concentrations are closer to
323 previously reported values in vertical snow and ice-core layers (e.g., Doherty et al., 2010 and
324 Polashenski et al., 2015). The overall higher concentrations of rBC in visibly darker patches,
325 where higher concentrations of ice algae were observed (Stibal et al., 2017), suggest potential bio
326 flocculation with ice algae and mineral dust. However, NAAPS model results also indicate the
327 increase is likely related to accumulation of episodically deposited wildfire-derived smoke. For
328 example, the smoke event in early August, which brought smoke from the western Northern
329 Hemisphere. Based on NAAPS deposition model and corroborated by rBC observations, wet
330 deposition appears to be the largest source of rBC to the surface. For example, our fresh snow
331 sample was measured at 3 μg-rBC/L-H_2O, while the model, off by a factor of 7, produced 21 μg-
332 rBC/L-H_2O. These preliminary results suggest global aerosol models may be overestimating BC
333 deposition; however, further investigation is warranted. These data provide utility in
334 understanding the seasonal evolution of impurities, which are needed to constrain modeling of
335 ice-albedo feedbacks in the bare-ice zone of the GRIS.
336
337 **Author Contributions**

ALK and JS analyzed the rBC samples. PX ran the NAAPS model and provided output data. ALK wrote the manuscript and PX and JS edited and contributed text. The samples were collected by ALK and the Dark Snow Project.

Acknowledgements

The authors thank the Dark Snow Project for field support and additional sample collection, specifically, M. Stibal, J. Box and K. Cameron and N. Molotch.

Competing Interests. There are no conflicts of interest.

Data Availability

The rBC and NAAPS modeled deposition data are included in Table 1.

References

Baumgardner, D., Popovicheva, O., Allan, J., Bernardoni, V., Cao, J., Cavalli, F ... & Viana, M.: Soot reference materials for instrument calibration and intercomparisons : a workshop summary with recommendations. 1869–1887. doi:10.5194/amt-5-1869-2012, 2012.

Bond, T. C., Doherty, S. J., Fahey, D. W., Forster, P. M., Berntsen, T., DeAngelo, B. J. ... & Zender, C. S: Bounding the role of black carbon in the climate system: A scientific assessment. *J. Geophys. Res. Atmos.* 118, 5380–5552. doi:10.1002/jgrd.50171, 2013.

Cordero, R. R., Sepúlveda, E., Feron, S., Damiani, A., Fernandoy, F., Neshyba, S., ... & Casassa, G. Black carbon footprint of human presence in Antarctica. *Nature communications*, *13*(1), 1-11, 2022.

Doherty, S. J., Grenfell, T. C., Forsström, S., Hegg, D. L., Brandt, R. E., and Warren, S. G.: Observed vertical redistribution of black carbon and other insoluble light-absorbing particles in melting snow. *J. Geophys. Res. Atmos.* 118, 5553–5569. doi:10.1002/jgrd.50235, 2013.

Doherty, S. J., Warren, S. G., Grenfell, T. C., Clarke, a. D., and Brandt, R. E.: Light-absorbing impurities in Arctic snow. *Atmos. Chem. Phys.* 10, 11647–11680. doi:10.5194/acp-10-

11647-2010, 2010.

Flanner, M. G., Zender, C. S., Randerson, J. T., and Rasch, P. J.: Present-day climate forcing and response from black carbon in snow. *J. Geophys. Res.* 112, D11202. doi:10.1029/2006JD008003, 2007.

Greuell, W.: Melt-water accumulation on the surface of the Greenland ice sheet: Effect on albedo and mass balance. *Geogr. Ann. Ser. A Phys. Geogr.* 82, 489–498. doi:10.1111/j.0435-3676.2000.00136.x, 2000.

Hanna, E., Huybrechts, P., Steffen, K., Cappelen, J., Huff, R., Shuman, C. .. & Griffiths, M: Increased runoff from melt from the Greenland Ice Sheet: A response to global warming. *J. Clim.* 21, 331–341. doi:10.1175/2007JCLI1964.1, 2008.

Katich, J. M., A. E. Perring, and J. P. Schwarz.: Optimized detection of particulates from liquid samples in the aerosol phase: focus on black carbon, *Aeros. Sci. Technol.*, doi:10.1080/02786826.2017.1280597, 2017.

Keegan, K. M., Albert, M. R., Mcconnell, J. R., and Baker, I.: Climate change and forest fires synergistically drive widespread melt events of the Greenland Ice Sheet. 1–4. doi:10.1073/pnas.1405397111, 2014.

Khan, A. L., H. Dierssen, J. P. Schwarz, C. Schmitt, A. Chlus, M. Hermanson, T. H. Painter, and D. M. M.: Impacts of coal dust on the spectral reflectance of Arctic surface snow in Svalbard, Norway, *Journal of Geophysical Research: Atmospheres*, 1–12. doi:10.1002/2016JD025757, 2017a.

Khan, A.L., Wagner, S., Jaffe, R., Xian P. , Williams M., and Armstrong, R., and McKnight, D.: Dissolved black carbon in the global cryosphere: Concentrations and chemical signatures, *Geophysical Research Letters*, 1–9. doi:10.1002/2017GL073485, 2017b.

389 Khan, A. L., McMeeking, G. R., Schwarz, J. P., Xian, P., Welch, K. A., Berry Lyons, W., &
390 McKnight, D. M.: Near-surface refractory black carbon observations in the atmosphere
391 and snow in the McMurdo dry valleys, Antarctica, and potential impacts of Foehn
392 winds. *J. Geophys. Res. Atmos.*, *123*(5), 2877-2887, 2018.
393 Khan, A. L., Klein, A. G., Katich, J. M., & Xian, P.: Local emissions and regional wildfires
394 influence refractory black carbon observations near Palmer Station, Antarctica. *Frontiers in*
395 *Earth Science*, *7*, 49, https://doi.org/10.3389/feart.2019.00049, 2019.
396 Khan, A. L., Rittger, K., Xian, P., Katich, J. M., Armstrong, R. L., Kayastha, R. B., ... &
397 McKnight, D. M.: Biofuel burning influences refractory black carbon concentrations in
398 seasonal snow at lower elevations of the Dudh Koshi River Basin of Nepal. *Frontiers in*
399 *Earth Science*, *8*, 371, https://doi.org/10.3389/feart.2020.00371, 2020.
400 Lewis, G., Osterberg, E., Hawley, R., Marshall, H. P., Meehan, T., Graeter, K. ... & Dibb, J:
401 Atmospheric blocking drives recent albedo change across the western Greenland ice sheet
402 percolation zone. Geophysical Research Letters, 48, e2021GL092814.
403 https://doi.org/10.1029/2021GL092814, 2021.
404 Lim, S., Faïn, X., Zanatta, M., Cozic, J., Jaffrezo, J.-L., Ginot, P., and Laj, P..: Refractory black
405 carbon mass concentrations in snow and ice: method evaluation and inter-comparison with
406 elemental carbon measurement. *Atmos. Meas. Tech.* 7, 3549–3589. doi:10.5194/amtd-7-
407 3549-2014, 2014.
408 Lynch, P., Reid, J. S., Westphal, D. L., Zhang, J., Hogan, T. F., Hyer, E. J., Curtis, C. A., Hegg,
409 D. A., Shi, Y., Campbell, J. R., Rubin, J. I., Sessions, W. R., Turk, F. J., and Walker, A. L.:
410 An 11-year global gridded aerosol optical thickness reanalysis (v1.0) for atmospheric and
411 climate sciences, Geosci. Model Dev., 9, 1489–1522, https://doi.org/10.5194/gmd-9-1489-
412 2016, 2016.

Markowicz, K. M., Pakszys, P., Ritter, C., Zielinski, T., Udisti, R., Cappelletti, D., ... & Karasiński, G.: Impact of North American intense fires on aerosol optical properties measured over the European Arctic in July 2015, J. Geophys. Res. Atmos., 121, 14,487–14,512, doi:10.1002/2016JD025310, 2016.

Markowicz, K.M., Lisok, J., and Xian, P., Simulation of long-term direct aerosol radiative forcing over the arctic within the framework of the iAREA project, Atmospheric Environment, doi: https://doi.org/10.1016/j.atmosenv.2020.117882, 2021.

McConnell, J. R., Edwards, R., Kok, G. L., Flanner, M. G., Zender, C. S., Saltzman, E. S., ... & Kahl, J. D.: 20th-century industrial black carbon emissions altered arctic climate forcing. *Science*, *317*(5843), 1381-1384, 2007.

Mori, T., Goto-Azuma, K., Kondo, Y., Ogawa-Tsukagawa, Y., Miura, K., Hirabayashi, M., ... & Nagatsuka, N.: Black Carbon and Inorganic Aerosols in Arctic Snowpack. *J. Geophys. Res. Atmos.*, 2019JD030623. doi:10.1029/2019JD030623, 2019.

Polashenski, C. M., Dibb, J. E., Flanner, M. G., Chen, J. Y., Courville, Z. R., Lai, A. M. …and Bergin, M.: Neither dust nor black carbon causing apparent albedo decline in Greenland's dry snow zone: Implications for MODIS C5 surface reflectance. 9319–9327. doi:10.1002/2015GL065912, 2015.

Ranjbar, K., O'Neill, N. T., Lutsch, E., McCullough, E. M., AboEl-Fetouh, Y., Xian, P. & Abboud, I.: Extreme smoke event over the high Arctic. *Atmos. Environ.* 218, 117002. doi:https://doi.org/10.1016/j.atmosenv.2019.117002, 2019.

Reid, J. S., Koppmann, R., Eck, T. F., and Eleuterio, D. P.: A review of biomass burning emissions part II: intensive physical properties of biomass burning particles, Atmos. Chem. Phys., 5, 799–825, https://doi.org/10.5194/acp-5-799-2005, 2005.

436 Ryan, J. C., Hubbard, A., Stibal, M., Irvine-Fynn, T. D., Cook, J., Smith, L. C.: Dark zone of the
437 Greenland Ice Sheet controlled by distributed biologically-active impurities. *Nat. Commun.*
438 9, 1–10. doi:10.1038/s41467-018-03353-2, 2018.
439 Ryan, J. C., Smith, L. C., Van As, D., Cooley, S. W., Cooper, M. G., Pitcher, L. H., …and Box,
440 J.: Greenland Ice Sheet surface melt amplified by snowline migration and bare ice exposure.
441 *Sci. Adv.* 5, 1–11. doi:10.1126/sciadv.aav3738, 2019.
442 Schwarz, J. P., Doherty, S. J., Li, F., Ruggiero, S. T., Tanner, C. E., Perring, A. E. …& Fahey,
443 D. W: Assessing recent measurement techniques for quantifying black carbon concentration
444 in snow. *Atmos. Meas. Tech. Discuss.* 5, 3771–3795. doi:10.5194/amtd-5-3771-2012, 2012.
445 Schwarz, J. P., Gao, R. S., Perring, a E., Spackman, J. R., and Fahey, D. W.: Black carbon
446 aerosol size in snow. *Sci. Rep.* 3, 1356. doi:10.1038/srep01356, 2013.
447 Stibal, M., Box, J. E., Cameron, K. A., Langen, P. L., Yallop, M. L., M., H., R., Khan, A.L.,
448 Molotch, N. P., Chrismas, N.A.M., Quaglia, F.C., , Remias, D., Paul, C.J.P., Van den
449 Broeke, M., Ryan, J.,, Hubbard, A.,, Tranter, M., van As, D., and and Ahlstrøm, A.: Algae
450 Drive Enhanced Darkening of Bare Ice on the Greenland Ice Sheet. *Geophys. Res. Lett.*,
451 463–471. doi:10.1002/2017GL075958, 2017.
452 Stibal, M., Elster, J., Šabacká, M., and Kaštovská, K. Seasonal and diel changes in
453 photosynthetic activity of the snow alga Chlamydomonas nivalis (Chlorophyceae) from
454 Svalbard determined by pulse amplitude modulation fluorometry. *FEMS Microbiol. Ecol.*
455 59, 265–273. doi:10.1111/j.1574-6941.2006.00264.x, 2007.
456 Tedesco, M., Doherty, S., Fettweis, X., Alexander, P., Jeyaratnam, J., & Stroeve, J.: The
457 darkening of the Greenland ice sheet: trends, drivers, and projections (1981–2100). *The*
458 *Cryosphere*, *10*(2), 477-496, 2016.

Wendl, I. A., Menking, J. A., Färber, R., Gysel, M., Kaspari, S. D., Laborde, M. J. G., & Schwikowski, M.: Optimized method for black carbon analysis in ice and snow using the Single Particle Soot Photometer. *Atmospheric Measurement Techniques*, *7*(8), 2667-2681, 2014.

Wientjes, I. G. M., Van De Wal, R. S. W., Reichart, G. J., Sluijs, A., and Oerlemans, J.: Dust from the dark region in the western ablation zone of the Greenland ice sheet. *Cryosphere* 5, 589–601. doi:10.5194/tc-5-589-2011, 2011.

Xian, P., Zhang, J., O'Neill, N. T., Toth, T. D., Sorenson, B., Colarco, P. R., Kipling, Z., Hyer, E. J., Campbell, J. R., Reid, J. S., and Ranjbar, K.: Arctic spring and summertime aerosol optical depth baseline from long-term observations and model reanalyses – Part 1: Climatology and trend, Atmos. Chem. Phys., 22, 9915–9947, https://doi.org/10.5194/acp-22-9915-2022, 2022.

Xian, P., Zhang, J., O'Neill, N. T., Reid, J. S., Toth, T. D., Sorenson, B., Hyer, E. J., Campbell, J. R., and Ranjbar, K.: Arctic spring and summertime aerosol optical depth baseline from long-term observations and model reanalyses – Part 2: Statistics of extreme AOD events, and implications for the impact of regional biomass burning processes, Atmos. Chem. Phys., 22, 9949–9967, https://doi.org/10.5194/acp-22-9949-2022, 2022.